RESEARCH ARTICLE

A Non-Equilibrium Atomic-Scale Simulation for Time-Evolutional Spin Dynamics of a Radical Bridged Trinuclear Ni(II) Complex

Aristide Colin,[a,b] Kenta Imoto,*[a] Marie Yoshikiyo,[a] Asuka Namai,[a] Masamichi Nishino,[c] Seiji Miyashita,[d] Talal Mallah,[b] and Shin-ichi Ohkoshi*[a,e]

Abstract: A non-equilibrium atomic-scale simulation for time-evolutional spin dynamics on molecular magnets is important to develop quantum electronic devices based on spin clusters and single molecule magnets. Herein we show spin dynamic calculations of individual spins in a radical-bridged trinuclear Ni(II) complex using the stochastic Landau-Lifshitz-Gilbert (s-LLG) model, involving superexchange interactions (J_{ij}) of spins between Ni (S= 1) cations (Ni1, Ni2, Ni3) and a hexahydroxytriphenylene (HHTP) radical (S= 1/2), and single-ion magnetic anisotropy (D_i) of Ni. The time-evolution simulation reveals the spin directions show damping oscillation within ~10 ps. At equilibrium, the spins are almost in the aromatic HHTP radical plane (*xy*-plane). The angles of the spins on Ni1, Ni2, Ni3, and the radical relative to the *x*-axis are 23.6°, 86.0°, 30.1°, and 31.4°, respectively, mainly due to negative D_{Ni1} value. The oscillation frequencies of 120 GHz and 210 GHz correspond to the zero-field magnetic resonance. Temperature-evolution simulations reveal the directions of the spins gradually fluctuate with increasing temperature, and finally the spins are almost randomly oriented above 5 K, reflecting the energy barrier by the total magnetic anisotropy. Such non-equilibrium atomic-scale simulations of time- and temperature-evolution dynamics would be useful for predicting qubit or coherence state of single molecule magnets.

Introduction

Control of the magnetic exchange coupling in polynuclear molecular complexes can be of interest for potential applications in the field of quantum information, in which coherence time and quantum gate properties are essential factors. Particularly, non-innocent bridging increased magnetic exchange coupling between magnetic ions[13–21], or control of the magnetic exchange interaction. Controlling the magnetic exchange interaction can be of interest for potential applications in the field of quantum information. Indeed, switching of the exchange interaction between magnetic ions behaving as qubits can entangle them, thus forming a quantum gate[22,23]. Examples of drastic modulation of the exchange coupling in dinuclear complexes[24–29] and more recently in trinuclear complexes[30–32] have been reported. For trinuclear complexes, the highly conjugated tris-dioxolene 2,3,6,7,10,11-hexahydroxytriphenylene (HHTP) bridging ligand has been used in the field of two-dimensional covalent metal-organic-frameworks or in several molecular complexes[33–43].A trinuclear molecular complex [{Ni(HBTp^{Ph,Ph})}$_3$(HHTP•)] (HBTp^{Ph,Ph}=tris(3,5diphenyl-1H-pyrazol-1-yl)(hydridoborate)) was synthesized in 2019[43]. This molecule exhibits electrochemical properties with five reversibly accessible oxidation states (Fig. S1). The charge neutral state, [{Ni(HBTp^{Ph,Ph})}$_3$(HHTP•)], was obtained as single crystals enabling analysis of the crystal structure as shown in Fig. 1a. There are three pentacoordinated Ni(II) ions, Ni1, Ni2, and Ni3. Ni1 adopts a trigonal bipyramidal geometry while Ni2 and Ni3 have square pyramidal geometries. In the neutral state, the HHTP ligand is in the tris-semiquinone state, {sq-sq-sq}•$^{3-}$, with three single electrons in interaction. Multireference ab initio computations for this neutral state showed that HHTP adopts a doublet ground state, where two of the electrons form a pair leaving one electron as a radical[44]. Molecular orbitals showed that the radical localizes near the Ni3 site (Fig. 1b and S2). Such asymmetric coordination originates from the difference in the

[a] A. Colin, K. Imoto, M. Yoshikiyo, A. Namai, S. Ohkoshi
Department of Chemistry, School of Science
The University of Tokyo
7-3-1 Hongo, Bunkyo-ku, Tokyo 113-0033, Japan
E-mail: imoto@chem.s.u-tokyo.ac.jp, ohkoshi@chem.s.u-tokyo.ac.jp
[b] A. Colin, T. Mallah
Institut de Chimie Moléculaire et des Matériaux d'Orsay, CNRS
Université Paris-Saclay
17 Avenue des Sciences, 91400 Orsay, France
[c] M. Nishino
Research Center for Materials Nanoarchitectonics
National Institute for Materials Science
1-1 Namiki, Tsukuba, Ibaraki 305-0044, Japan
[d] S. Miyashita
JSR-UTokyo Collaboration Hub, CURIE, Department of Physics
The University of Tokyo
7-3-1 Hongo, Tokyo 113-0033, Japan
[e] S. Ohkoshi
CNRS International Research Laboratory DYNACOM
7-3-1 Hongo, Bunkyo-ku, Tokyo 113-0033, Japan

Supporting information for this article is given via a link at the end of the document.

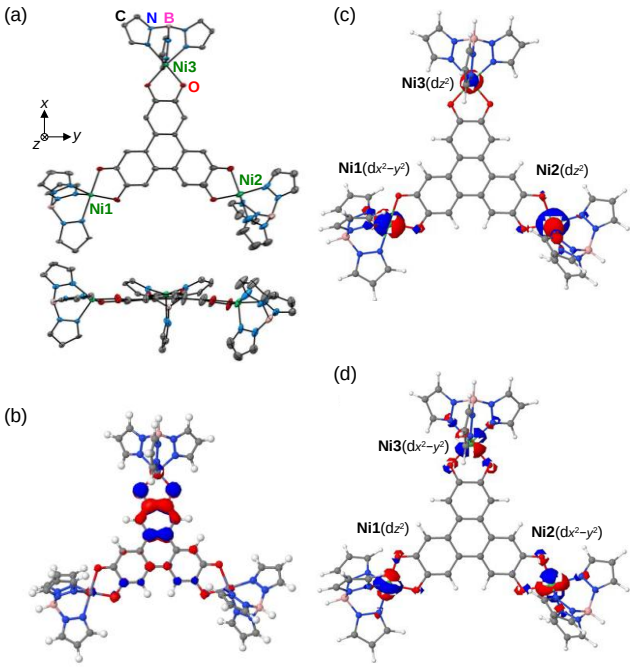


Figure 1. (a) Top view (upper) and side view (lower) of the molecular structure of [{Ni(HBTpPh,Ph)}$_3$(HHTP•)] obtained from single crystal analysis in ref. 43. Ni, N, O, C, and B atoms are represented as green, light blue, red, gray, and pink, respectively. Functional groups on trispyrazolylborate ligands are omitted for clarity. (b) Magnetic orbital of HTTP radical and (c,d) those of d-orbitals of Ni adapted from ref. 44. It is noted that Fig. 1b is the calculated result of the Zn analogue of the present system.

coordination environments of the three Ni(II) sites and the non-planar structure of the HHTP ligand that breaks the C_3 symmetry. As for the d-orbitals of the Ni(II) ions, Ni1 possesses its single-ion anisotropy axis in the triangular plane. On the other hand, the anisotropy axes of Ni2 and Ni3 are perpendicular to the triangular plane. Figures 1c and 1d show the representative d-orbitals of the three Ni(II) sites. In the present work, we show the non-equilibrium atomic-scale simulation of the time-evolution spin dynamics for the relaxation process to the equilibrium spin configuration of [{Ni(HBTp^{Ph,Ph})}$_3$(HHTP•)] with a visualization of the individual spins by the stochastic Landau-Lifshitz-Gilbert (sLLG) calculations, and temperature-evolution of spin dynamics under the effect of thermal fluctuations.

Results and Discussion

Calculation Process of Non-Equilibrium Atomic-Scale Simulations of Spin Dynamics

In the present calculation, we applied the following spin Hamiltonian,

$$\mathcal{H} = -\sum_{\langle i,j \rangle} J_{i,j} \boldsymbol{S_i} \cdot \boldsymbol{S_j} + \sum_i \boldsymbol{S_i} \mathcal{D}_i \boldsymbol{S_i} - g_i \beta \boldsymbol{H} \cdot \sum_i \boldsymbol{S_i} \ ,$$

where $J_{i,j}$ is the superexchange interaction between the *i* and *j* sites, $\boldsymbol{S_i}$ (or $\boldsymbol{S_j}$) is the spin angular momentum of the *i* (or *j*) site, $\mathcal{D}_i$ is the anisotropy tensor for the *i* site, $\boldsymbol{H}$ is the magnetic field applied to *i* site, g_i is *g* value for the *i* site, and β is Bohr magneton. For theoretical calculations of the magnetic system, thermal fluctuations were taken into account by introducing the thermal noise to Landau-Lifshitz-Gilbert equation as random noise into the effective field ($\boldsymbol{H_i^{eff}} \rightarrow \boldsymbol{H_i^{eff}} + \boldsymbol{\xi_i}$), resulting in the sLLG equation,[45–47]

$$\frac{d}{dt}\boldsymbol{S_i} = -\frac{\gamma_i}{1+\alpha_i^2}\boldsymbol{S_i} \times \left(\boldsymbol{H_i^{eff}} + \boldsymbol{\xi_i}\right) - \frac{\gamma_i}{(1+\alpha_i^2)|\boldsymbol{S_i}|}\boldsymbol{S_i} \times \left[\boldsymbol{S_i} \times \left(\boldsymbol{H_i^{eff}} + \boldsymbol{\xi_i}\right)\right],$$

where $\boldsymbol{S_i}$ is the magnetization of *i* site, α_i is the damping factor of *i* site, $\gamma_i (= g_i\beta/\hbar)$ is gyromagnetic constant, $\boldsymbol{\xi_i}$ is the white Gaussian noise applied at *i* site, and $\boldsymbol{H_i^{eff}}$ is the effective field calculated from the derivative of the Hamiltonian as

$$g_i \beta \boldsymbol{H_i^{eff}} = -\frac{\partial}{\partial \boldsymbol{S_i}} \mathcal{H}(\boldsymbol{S_1} \cdots \boldsymbol{S_n}, t).$$

$\boldsymbol{\xi_i}(t)$ satisfies the following relations: $\langle \xi_i^\mu(t) \rangle = 0$, $\langle \xi_i^u(t) \xi_j^v(t') \rangle = 2A_i \delta_{ij} \delta_{uv} \delta(t-t')$, where *u* and *v* are the Cartesian components and A_i is the amplitude of the noise, which is expressed as $A_i = \alpha_i k_B T / \gamma_i |\boldsymbol{S_i}|$ to assure the canonical distribution in the equilibrium state[47].

In the present simulation, we used the magnetic interaction parameters of [{Ni(HBTp^{Ph,Ph})}$_3$(HHTP•)] (hereafter HHTP• is referred to as R•) reported in the previous literature[44]. Fig. S3 shows the crystal structure, which contains two molecules in the unit cell. Spins are set on each of the three Ni(II) sites as *S*=1 and on R• as *S*=1/2. Based on the calculations performed in the

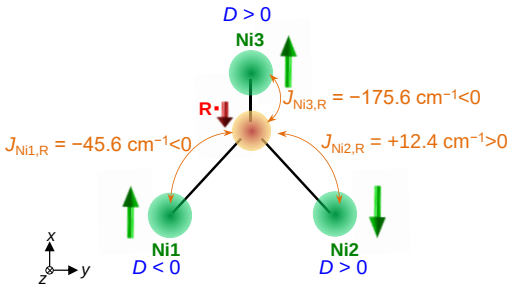


Figure 2. (a) Top view (upper) and side view (lower) of the molecular structure of [{Ni(HBTpPh,Ph)}$_3$(HHTP•)] obtained from single crystal analysis in ref. 43. Ni, N, O, C, and B atoms are represented as green, light blue, red, gray, and pink, respectively. Functional groups on trispyrazolylborate ligands are omitted for clarity. (b) Magnetic orbital of HTTP radical and (c,d) those of d-orbitals of Ni adapted from ref. 44. It is noted that Fig. 1b is the calculated result of the Zn analogue of the present system.

previous paper[44], the superexchange interaction between the Ni sites (Ni1, Ni2, and Ni3) and R• are set as $J_{Ni1,R}$, $J_{Ni2,R}$, and $J_{Ni3,R}$, respectively, and the anisotropy tensor ($\mathcal{D}_i$) for the Ni sites were set as shown in Fig. 2, Fig. S4 and Table S1. The anisotropy tensor elements including off-diagonal anisotropy terms used in the present study are listed in Table S2. *g* value is assume to isotropic value of 2.3 for all Ni sites.[44] Since we do not have experimental or theoretical evidence of the α value for the target system, in the present calculation, to calculate fast relaxation process, α value was fixed to 0.1, which is the largest practical value described in the previous literature.[45]

Time-Evolutional Spin Dynamics

The time-evolution of spin dynamics was performed by calculating at 0.0001 K (nearly equal to 0 K) under zero magnetic field (H= 0). The initial spins were set to be parallel along the *x*-axis in-plane of the planar HHTP molecule at 0 ps as shown in Fig. 2. Ni1 and Ni3 are parallelly oriented towards the +*x* direction, while Ni2 and R• are antiparallelly oriented towards the −*x* direction. The simulation revealed that the spin directions tilt to the *y*-axis direction with damping oscillation over a time span of 15 ps as shown in Fig 3a. Supporting Movie 1 shows the relaxation process. The spin on Ni1 relaxed to its equilibrium within 5 ps, while the spins on Ni2, Ni3, and R• relaxed within 15 ps (Fig. 3). At equilibrium, the directions of the spins on all sites are almost in the *xy*-plane, i.e., the angle (φ) from the aromatic HHTP radical plane (*xy*-plane) are φ= 3.5° for Ni1, φ= 6.0° for Ni2, φ= 15.6° for Ni3, and φ= 13.0° for R•. In the *xy*-plane, the rotation angle from the spins on Ni1, Ni2, Ni3, and R• in respect to the *x*-axis (θ) are θ= 23.6°, 86.0°, 30.1°, and 31.4°, respectively. Such an equilibrium spin configuration indicates that the orientations of spins are governed by the direction of negative D_{Ni1} (magnetic easy axis). It is noted that the above configuration is confirmed as the most stable by obtaining the same configuration in the simulations starting from the randomly selected 513 configurations and sweeping the temperature from 20 K to 0.0001 K with 1 K ns^{-1} (Fig. S5). Additionally, the simulations with α values of 0.02 and 0.05 resulted in the convergence to the same configuration (Fig. S6).

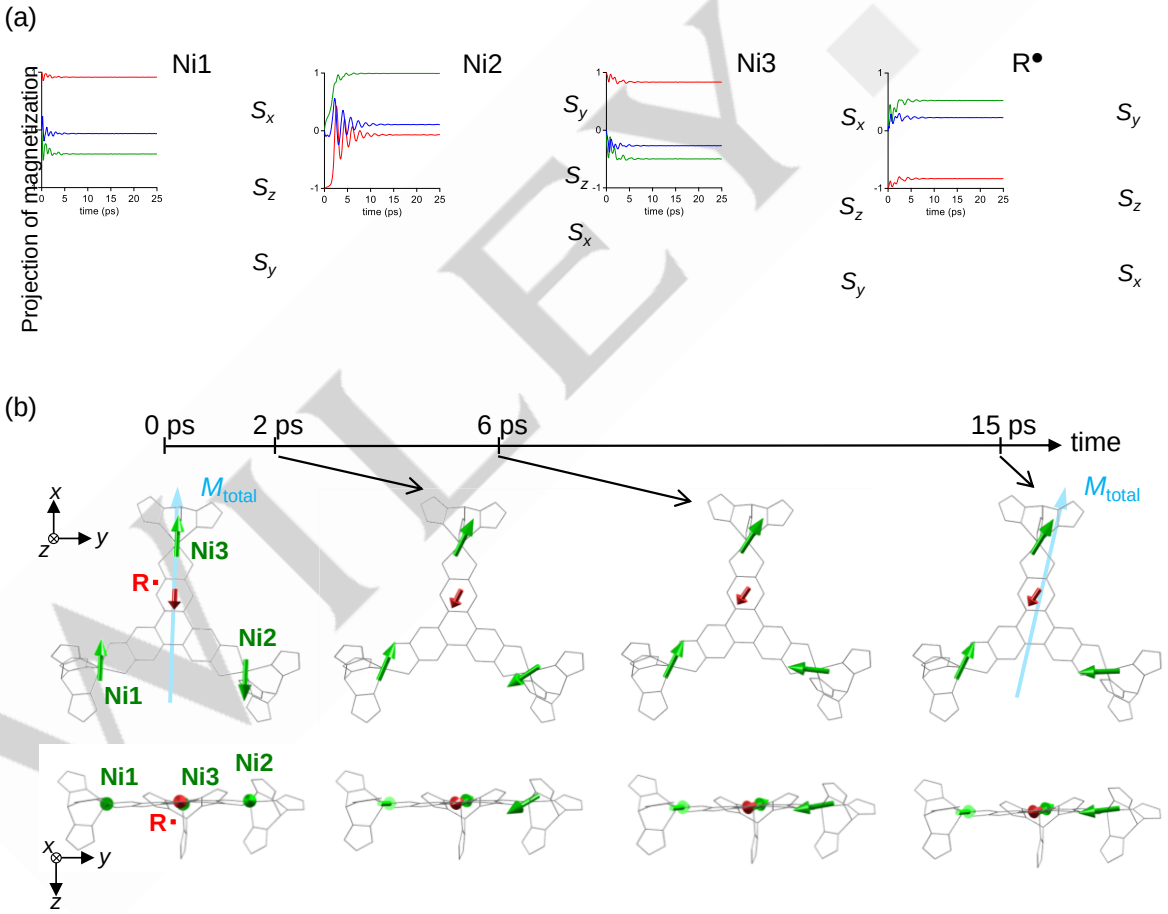


Figure 3. (a) Temporal evolution of the magnetization projected along each crystallographic axis. Red, green, and blue lines represent magnetic moments along the *a*, *b*, and *c*-axes, respectively. (b) Spin configurations at 0 ps, 2 ps, 6 ps, and 15 ps. Green and red arrows represent the spins on Ni and R•, respectively. Light blue arrows are the directions of the total magnetization.

Concerning the damping oscillation of the relaxation process, we evaluated the frequency of the damping oscillation by the fast Fourier transform (FFT) over 0–400 ps (Fig. 4). The FFT result indicates that the spin on Ni1 primarily oscillate at 210 GHz, while the spin on Ni2 oscillates strongly with a frequency of 120 GHz, and the spins on Ni3 and R• oscillate at both 120 GHz and 210 GHz. These frequencies are considered to correspond to the zero-field magnetic resonances of the present system.

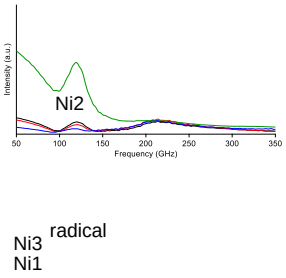


Figure 4. Frequency of spin oscillations for Ni1 (blue), Ni2 (green), Ni3 (red), and R• (black) during the relaxation process towards the equilibrium configuration.

Temperature-Dependence of Spin Dynamics

Next, we evaluated the thermal fluctuation of the spins in the present system. With increasing temperature, the spins start to deviate from their equilibrium states. First, let us look at the status at 2 K. At 2 K, Ni1 fluctuates around its magnetic easy axis (+z_{Ni1}-axis), while Ni2 and Ni3 fluctuate within their magnetic easy-planes ($x_{Ni2}y_{Ni2}$-plane and $x_{Ni3}y_{Ni3}$-plane, respectively) (Fig. 5). The spin on Ni1 orient to one direction, while the spins on R•, Ni2, and Ni3 are spread in a fan-like form. At 5 K, the spins on Ni1, Ni3, and R• also appear at the opposite direction as shown in the bow-tie-shaped distribution in Fig. 5. At 20 K, the directions of the spins are no longer pinned to specific directions, and the spins on R•, Ni2, and Ni3 show spherical distributions. Supporting Movies 2 and 3 show the direction of the trinuclear molecule within the unit cell, respectively.

Conclusion

In conclusion, we calculated and visualized the spin dynamics of [{Ni(HBTp^{Ph,Ph})}$_3$(HHTP)]•, and revealed the relaxation process to the equilibrium magnetic configuration as well as the fluctuation of the spins by the effect of temperature. This work is a unique trial to carry out sLLG simulations of the dynamics of individual spins in a metal complex containing both radicals and magnetic ions. The sLLG method is a powerful tool since it is capable of simulating the dynamics of individual spins in response to temperature, external magnetic field, and electromagnetic waves. Such simulations applicable to single molecule magnets or metal complexes, which have potential for future spin qubits, will give insights into the development of spin materials.

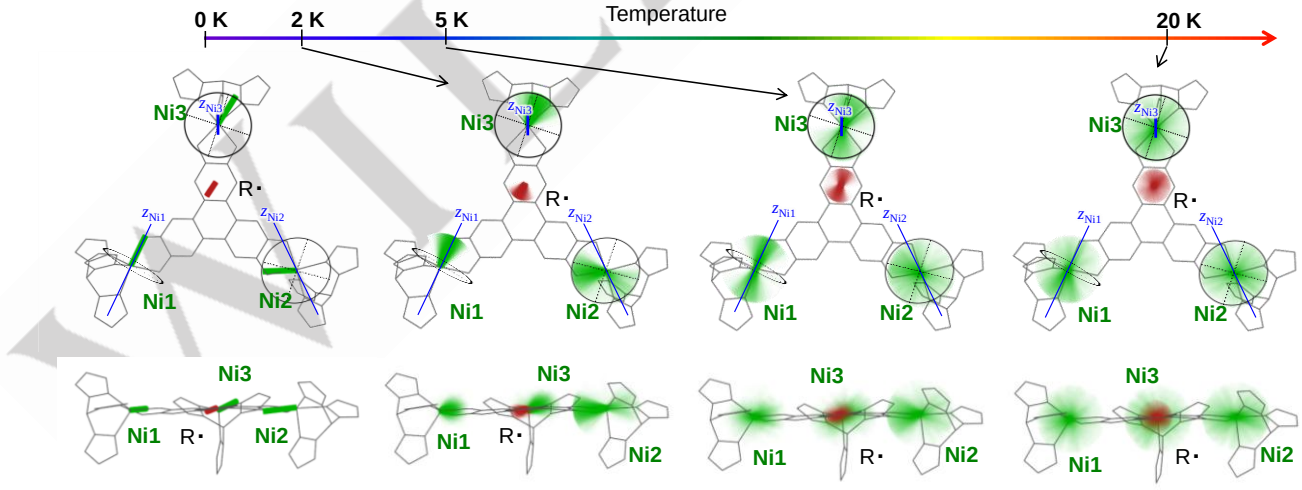


Figure 5. Diagram showing the distribution of the spin directions at 0.0001 K, 2 K, 5 K, and 20 K, composed by overlay of snapshots of the spins between 0–100 ps. Upper are top views from the *z*-axis direction, and lower are the side views. Green and red colors indicate the spin directions of Ni and R•, respectively. Blue bars show the $z_{Ni1,Ni2,Ni3}$-axes of the single-ion anisotropy at the Ni1,2,3 sites.

Acknowledgements

This work was supported by Grant-in-Aid for Scientific Research (A) from the Japan Society for the Promotion of Science (JSPS) (20H00369), IRL DYNACOM of CNRS, CNRS – University of Tokyo "Excellence Science" Joint Research Program, and Second CNRS – University of Tokyo PhD Joint Program, a JSPS Grant-in-Aid for Scientific Research B (23H01920), Scientific Research B (24K01332), Scientific Research C (23K04688), and Young Scientists (JP24K17606), JST SPRING (JPMJSP2108), and Joint PhD Programme of Université Paris-Saclay as part of the «Investissements d'Avenir» program (ANR-11-IDEX-003).

Keywords: Spin dynamics calculations • Molecule-based magnet • Stochastic Landau-Lifshitz-Gilbert (s-LLG) model

[1] A. Dei, D. Gatteschi, C. Sangregorio, L. Sorace, *Acc. Chem. Res.* **2004**, *37*, 827.

[2] D. N. Hendrickson and C. G. Pierpont, *Top. Curr. Chem.* **2004**, *234*, 63.

[3] E. Evangelio and D. Ruiz-Molina, *Eur. J. Inorg. Chem.* **2005**, *2005*, 2957.

[4] A. Beni, A. Dei, S. Laschi, M. Rizzitano and L. Sorace, *Chem. Eur. J.* **2008**, *14*, 1804.

[5] I. L. Fedushkin, O. V.Maslova, A. G. Morozov, S. Dechert, S., S. Demeshko and F. Meyer, *Angew. Chem. Int. Ed.* **2012**, *51*, 10584.

[6] K. G. Alley, G. Poneti, P. S. D. Robinson, A. Nafady, B. Moubaraki, J. B. Aitken, S. C. Drew, C. Ritchie, B. F. Abrahams, R. K. Hocking, K. S. Murray, A. M. Bond, H. H. Harris, L. Sorace and C. Boskovic, *J. Am. Chem. Soc.* **2013**, *135*, 8304.

[7] T. Tezgerevska, K. G. Alley and C. Boskovic, *Coord. Chem. Rev.* **2014**, *268*, 23.

[8] M. A. Dunstan, E. Rousset, M.-E. Boulon, R. W. Gable, L. Sorace and C. Boskovic, *Dalton Trans.* **2017**, *46*, 13756.

[9] J. Chen, Y. Sekine, Y. Komatsumaru, S. Hayami and H. Miyasaka, *Angew. Chem. Int. Ed.* **2018**, *57*, 12043.

[10] Y. Suenaga, T. Mibu, T. Okubo, M. Maekawa, T. Kuroda-Sowa and K. Sugimoto, *Dalton Trans.* **2021**, *50*, 9833.

[11] M. Wang, Z.-Y. Li, R. Ishikawa and M. Yamashita, *Coord. Chem. Rev.* **2021**, *435*, 213819.

[12] A. A. Kamin, I. P. Moseley, J. Oh, E. J. Brannan, P. M. Gannon, W. Kaminsky, J. M. Zadrozny and D. J. Xiao, *Chem. Sci.* **2023**, *14*, 4083.

[13] K. Chakarawet, T. D. Harris and J. R. Long, *Chem. Sci.* **2020**, *11*, 8196.

[14] S. Demir, J. M. Zadrozny, M. Nippe and J. R. Long, *J. Am. Chem. Soc.* **2012**, *134*, 18546.

[15] S. Demir, M. Nippe, M. I. Gonzalez and J. R. Long, *Chem. Sci.* **2014**, *5*, 4701.

[16] S. Demir, M. I. Gonzalez, L. E. Darago, W. J. Evans, J. R. Long, *Nat. Commun.* **2017**, *8*, 2144.

[17] J. D. Rinehart, M. Fang, W. J. Evans and J. R. Long, *J. Am. Chem. Soc.* **2011**, *133*, 14236.

[18] J. A. DeGayner, I.-R. Jeon and T. D. Harris, *Chem. Sci.* **2015**, *6*, 6639.

[19] J. J. Loughrey, N. J. Patmore, A. Baldansuren, A. J. Fielding, E. J. L. Mclnnes, M. J. Hardie S. Sproules and M. A. Halcrow, *Chem. Sci.* **2015**, *6*, 6935.

[20] C. Hua, J. A. DeGayner and T. D. Harris, *Inorg. Chem.* **2019**, *58*, 7044.

[21] B. S. Dolinar, S. Gómez-Coca, D. I. Alexandropoulos and K. R. Dunbar, *Chem. Comm.* **2017**, *53*, 2283.

[22] J. Lehmann, A. Gaita-Ariño, E. Coronado and D. Loss, *Nat. Nanotechnol.* **2007**, *2*, 312.

[23] J. Ferrando-Soria, S. A.Magee, A. Chiesa, S. Carretta, P. Santini, I. J. Vitorica-Yrezabal, F. Tuna, G. F. S. Whitehead, S. Sproules, K. M. Lancaster, A.-L. Barra, G. A. Timco, E. J. L. McInnes and R. E. P. Winpenny, *Chem.* **2016**, *1*, 727.

[24] K. S. Min, A. G. DiPasquale, J. A. Golen, A. L. Rheingold and J. S. Miller, *J. Am. Chem. Soc.* **2007**, *129*, 2360.

[25] J. S. Miller and K. S. Min, *Angew. Chem. Int. Ed.* **2009**, *48*, 262.

[26] X. Ma, E. A. Suturina, S. De, P. Négrier, M. Rouzières, R. Clérac and P. Dechambenoit, *Angew. Chem. Int. Ed.* **2018**, *57*, 7841.

[27] X. Ma, E. A. Suturina, M. Rouzières, M. Platunov, F. Wilhelm, A. Rogalev, R. Clérac and P. Dechambenoit, *J. Am. Chem. Soc.* **2019**, *141*, 7721.

[28] P. Zhang, M. Perfetti, M. Kern, P. P. Hallmen, L. Ungur, S. Lenz, M. R. Ringenberg, W. Frey, H. Stoll, G. Rauhut and J. van Slageren, *Chem. Sci.* **2018**, *9*, 1221.

[29] S. Suhr, D. Hunger, R. R. M. Walter, A. Köhn, J. van Slageren and B. Sarkar, *Inorg. Chem.* **2024**, *63*, 6042.

[30] L. Yang and M. Dincă, *Angew. Chem. Int. Ed.* **2021**, *60*, 23784.

[31] L. Yang, J. J. Oppenheim and M. Dincă, *Dalton Trans.* **2022**, *51*, 8583.

[32] J. A. Intrator, N. M. Orchanian, A. J. Clough, R. Haiges and S. C. Marinescu, *Dalton Trans.* **2022**, *51*, 5660.

[33] M. Hmadeh, Z. Lu, Z. Liu, F. Gándara, H. Furukawa, S. Wan, V. Augustyn, R. Chang, L. Liao, F. Zhou, E. Perre, V. Ozolins, K. Suenaga, X. Duan, B. Dunn, Y. Yamamoto, O. Terasaki and O. M. Yaghi, *Chem. Mater.* **2012**, *24*, 3511.

[34] G. Skorupskii, B. A. Trump, T. W. Kasel, C. M. Brown, C. H. Hendon and M. Dincă, *Nat. Chem.* **2020**, *12*, 131.

[35] Y. Misumi, A. Yamaguchi, Z. Zhang, T. Matsushita, N. Wada, M. Tsuchiizu and K. Awaga, *J. Am. Chem. Soc.* **2020**, *142*, 16513.

[36] T. Chen, J.-H. Dou, L. Yang, C. Sun, N. J. Libretto, G. Skorupskii, J. T. Miller and M. Dincă, *J. Am. Chem. Soc.* **2020**, *142*, 12367.

[37] X. Song, X. Wang, Y. Li, C. Zheng, B. Zhang, C. Di, F. Li, C. Jin, W. Mi, L. Chen and W. Hu, *Angew. Chem. Int. Ed.* **2020**, *59*, 1118.

[38] G. Skorupskii, K. N. Le, D. L. M. Cordova, L. Yang, T. Chen, C. H. Hendon, M. Q. Arguilla and M. Dincă, *P. Natl. A. Sci. USA*, **2022**, *119*, e2205127119.

[39] A. Ugale, P. Ninawe, A. Jain, M. Sangole, R. Mandal, K. Singh and N. Ballav, *Inorg. Chem.* **2024**, *63*, 3675.

[40] A. M. Barthram, R. L. Cleary, R. Kowallick and M. D. Ward, *Chem. Commun.* **1998**, *24*, 2695.

[41] Y. Suenaga, H. Inada, M. Inomata, R. Yamaguchi, T. Okubo, M. Maekawa and T. Kuroda-Sowa, *Chem. Lett.* **2014**, *43*, 562.

[42] L. Yang, X. He and M. Dincă, *J. Am. Chem. Soc.* **2019**, *141*, 10475.

[43] Y. Wang, F. Lambert, E. Rivière, R. Guillot, C. Herrero, A. Tissot, Z. Halime and T. Mallah, *Chem. Commun.* **2019**, *55*, 12336.

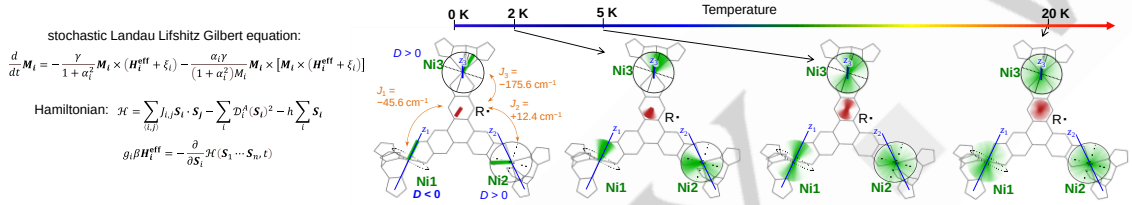
[44] N. Suaud, A. Colin, M. Bouammali, T. Mallah and N. Guihéry, *Chem. Eur. J.* **2024**, *30*, e202302256.

[45] H. Kronmüller and M. Fähnle, *Micromagnetism and the Microstructure of Ferromagnetic Solids*, Cambridge University Press, **2003**.

[46] G. Grinstein and R. H. Koch, *Phys. Rev. Lett.* **2003**, *90*, 207201.

[47] M. Nishino and S. Miyashita, *Phys. Rev. B* **2015**, *91*, 134411.

Entry for the Table of Contents



Spin dynamic calculations of individual spins in a radical-bridged trinuclear Ni(II) complex using the stochastic Landau-Lifshitz-Gilbert (s-LLG) model involving superexchange interactions (*J*) and single-ion anisotropy (*D*) revealed the temporal dynamics and the temperature fluctuation of spins, indicating the applicability of the methods for predicting qubit or coherence state of single molecule magnets.